

Chemisorption of acrylonitrile on the Cu(100) surface: A local density functional study

Xavier Crispin, C. Bureau, V. M. Geskin, R. Lazzaroni, William R. Salaneck and J. L. Bredas

Linköping University Post Print

N.B.: When citing this work, cite the original article.

Original Publication:

Xavier Crispin, C. Bureau, V. M. Geskin, R. Lazzaroni, William R. Salaneck and J. L. Bredas, Chemisorption of acrylonitrile on the Cu(100) surface: A local density functional study, 1999, Journal of Chemical Physics, (111), 7, 3237-3251.

<http://dx.doi.org/10.1063/1.479604>

Copyright: American Institute of Physics (AIP)

<http://www.aip.org/>

Postprint available at: Linköping University Electronic Press

<http://urn.kb.se/resolve?urn=urn:nbn:se:liu:diva-81301>

Chemisorption of acrylonitrile on the Cu(100) surface: A local density functional study

X. Crispin, C. Bureau, V. M. Geskin, R. Lazzaroni, W. R. Salaneck et al.

Citation: *J. Chem. Phys.* **111**, 3237 (1999); doi: 10.1063/1.479604

View online: <http://dx.doi.org/10.1063/1.479604>

View Table of Contents: <http://jcp.aip.org/resource/1/JCPSA6/v111/i7>

Published by the [American Institute of Physics](#).

Additional information on *J. Chem. Phys.*

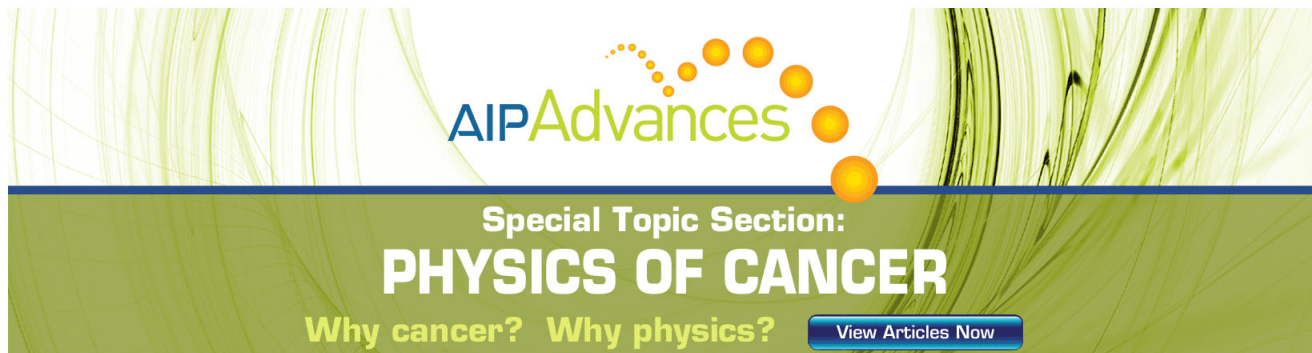
Journal Homepage: <http://jcp.aip.org/>

Journal Information: http://jcp.aip.org/about/about_the_journal

Top downloads: http://jcp.aip.org/features/most_downloaded

Information for Authors: <http://jcp.aip.org/authors>

ADVERTISEMENT



AIP Advances

Special Topic Section:
PHYSICS OF CANCER

Why cancer? Why physics? [View Articles Now](#)

Chemisorption of acrylonitrile on the Cu(100) surface: A local density functional study

X. Crispin

Service de Chimie des Matériaux Nouveaux, Centre de Recherche en Electronique et Photonique Moléculaires, Université de Mons-Hainaut, Place du Parc 20, B-7000 Mons, Belgium, and Department of Physics and Measurement Technology, Linköping University, S-58183 Linköping, Sweden

C. Bureau

DSM-DRECAM-SRSIM, bât.466 CEA-Saclay F-91191 Gif-sur-Yvette Cedex, France

V. M. Geskin and R. Lazzaroni

Service de Chimie des Matériaux Nouveaux, Centre de Recherche en Electronique et Photonique Moléculaires, Université de Mons-Hainaut, Place du Parc 20, B-7000 Mons, Belgium

W. R. Salaneck

Department of Physics and Measurement Technology, Linköping University, S-58183 Linköping, Sweden

J. L. Brédas^{a)}

Service de Chimie des Matériaux Nouveaux, Centre de Recherche en Electronique et Photonique Moléculaires, Université de Mons-Hainaut, Place du Parc 20, B-7000 Mons, Belgium

(Received 10 March 1999; accepted 21 May 1999)

The possibility of chemically grafting polyacrylonitrile onto transition metal electrodes via electropolymerization leads to promising applications in the fields of corrosion protection or metal surface functionalization. The initial step of the electrografting mechanism is the adsorption of the acrylonitrile monomer on the metal surface from solution. Here, we investigate theoretically this adsorption process on the copper (100) surface; Density Functional Theory is used in the Local Spin Density approximation to describe the electronic and structural properties of acrylonitrile adsorbed on copper clusters. The chemisorption of acrylonitrile on the copper surface is confirmed experimentally via X-Ray Photoelectron Spectroscopy. The thermodynamic characteristics of the adsorption process are also studied via statistical mechanics. Finally, determining the influence of the copper cluster size on the adsorption of acrylonitrile allows to extrapolate the properties of the acrylonitrile/Cu(100) surface from those of acrylonitrile/copper clusters. © 1999 American Institute of Physics. [S0021-9606(99)70231-X]

I. INTRODUCTION

In the context of catalysis and interfacial phenomena, cluster models are widely used to study theoretically the interaction between atoms or molecules and transition metal surfaces. From a chemical point of view, the cluster approach is justified by considering chemisorption as a local phenomenon where long-range interactions can be neglected. The advantages of finite models of metal surfaces are, on the one hand, that the adsorbate geometry is usually reliably calculated¹ and, on the other hand, that the limited extent of the system allows one to apply quantum-chemical studies at a sophisticated level, in order to determine the nature of the molecule/surface interaction. However, the size and shape of the metal clusters affect their electronic properties and consequently their reactivity.²⁻⁴ It is indeed well known theoretically^{2,3} as well as experimentally⁵ that the chemisorption energy of an adsorbate can vary dramatically with the size of transition metal clusters. The consequences are the following: first, it is not straightforward to relate the chemi-

sorption energy evaluated from cluster calculations to the chemisorption energy of an adsorbate on a true metal surface; second, any study of adsorption by means of finite models must tackle the influence of cluster size.

In this work, the adsorption of acrylonitrile (AN) on the Cu(100) surface is studied by considering model clusters for the copper surface. The size of the clusters is increased in order to observe its influence on AN adsorption and to understand the chemisorption of AN on the actual Cu(100) surface. The AN/cluster complexes are analyzed in terms of the following: adsorption geometry, vibrational properties, and charge transfer due to chemisorption. The chemisorption of AN on a copper surface and its partial charge transfer are confirmed by X-Ray Photoelectron Spectroscopy (XPS) results. The nature of the interaction is described in terms of molecular orbital mixing. An evaluation of the order of magnitude of the entropy loss upon chemisorption is proposed, which allows for an estimate of the free enthalpy of adsorption. To the best of our knowledge, the chemisorption energy of acrylonitrile on the (100) copper surface has not been reported experimentally.

The adsorption of acrylonitrile on oxide-free metallic

^{a)}Electronic mail: jeanluc@averell.umh.ac.be

electrodes appears as a key step in the mechanism^{1(e)} that leads to the formation of polyacrylonitrile films chemically grafted to metal electrodes during an electropolymerization process.^{6(a)} The interesting properties of such polymer films, in particular their high adherence and homogeneity, have generated intensive experimental⁶ as well as theoretical studies.⁷ Among the latter, various finite models of acrylonitrile or methacrylonitrile and transition metal surfaces were studied in order to rationalize the electrografting mechanism.^{1(e),4,8} The present work brings new advances in our understanding of the chemisorption of acrylonitrile on copper surfaces, based on a systematic comparison between theoretical results and experimental data: (i) the photoionization spectrum of Cu(100) is compared to the total density of states of copper clusters modeling the surface; (ii) the Surface-Enhanced Raman Scattering spectrum (SERS) of adsorbed acrylonitrile is compared with the calculated vibrational frequencies of an (acrylonitrile-copper cluster) complex; and (iii) the X-Ray Photoelectron Spectroscopy (XPS) data are related to the calculated chemisorption charge transfer between the metal surface model and acrylonitrile (note that a detailed XPS and UPS analysis of the chemisorption of acrylonitrile on copper and nickel surfaces will be described elsewhere).

II. METHODOLOGY

A. Molecular models

The adsorption of acrylonitrile on a Cu(100) surface is modeled by complexes composed of one acrylonitrile molecule interacting with a copper cluster. This “ultrahigh-vacuum-type” model is comparable to the adsorption of acrylonitrile from a solution to a clean metallic electrode set at its potential of zero charge. Our approach is thus relevant for describing the first step of electrografting experiments. Note that it has been verified experimentally⁹ that the electronic structure of a clean metal surface in an ultrahigh vacuum is very similar to that of the same metal in solution when set under its potential of zero charge.

A characteristic adsorption site on the (100) surface of the fcc copper crystal is modeled by various copper clusters with sizes ranging from 9 to 20 copper atoms (Fig. 1). The interatomic distances are fixed at the bulk crystal values, so that all reconstruction phenomena are neglected. The description of the electronic properties of these copper clusters has been detailed elsewhere.⁴

The clusters have two atomic layers; the smallest is Cu₉(5,4) (where the subscript indicates the total number of copper atoms in the cluster and the numbers between parentheses denote the composition of its layers: here, five atoms in the upper layer and four in the bottom layer), in which the central atom of the upper layer has the same number of nearest neighbors as on the actual (100) surface. In a previous study, Geskin *et al.*^{8(e)} showed that acrylonitrile adsorbed on Cu₉(5,4) is bound to two copper atoms (colored in dark in Fig. 1): the first one is the central atom and the second one is an edge atom of the cluster, which is unsaturated with respect to an actual surface atom. We have thus enlarged the surface models in order to saturate the second copper atom

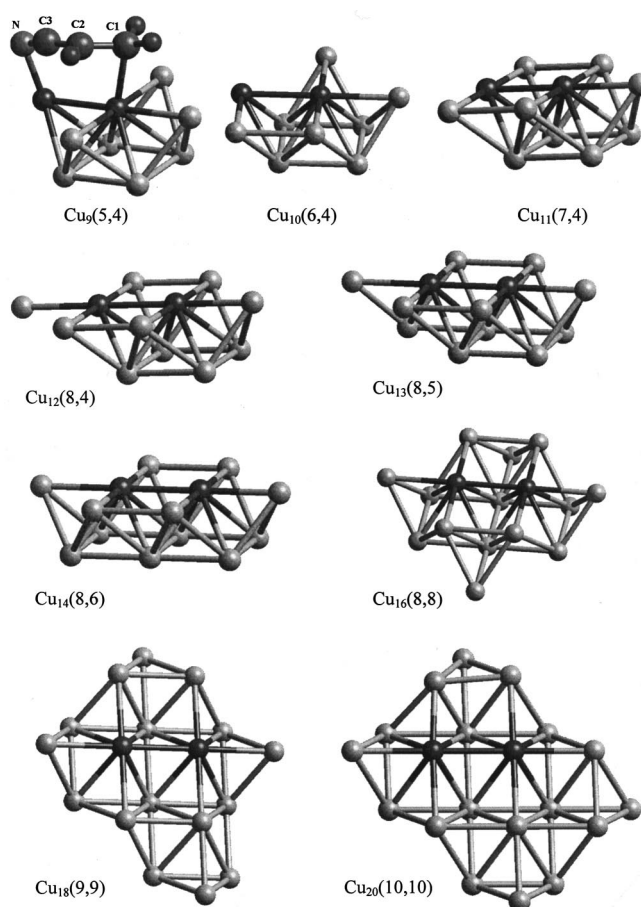


FIG. 1. Representation of the copper clusters $\text{Cu}_n(y,w)$ used as models of the Cu(100) surface. The clusters are composed of two atomic layers, where the upper layer contains y atoms and the other w atoms. The two copper atoms that are drawn in dark are those that are bonded to the chemisorbed acrylonitrile in all the $[\text{Cu}_n(y,w)-\text{AN}]$ complexes.

bound to acrylonitrile. This is done by extending the upper layer [$\text{Cu}_{10}(6,4)$, $\text{Cu}_{11}(7,4)$, $\text{Cu}_{12}(8,4)$] and the bottom layer [$\text{Cu}_{13}(8,5)$ and $\text{Cu}_{14}(8,6)$]. The latter cluster, $\text{Cu}_{14}(8,6)$, has two central atoms, which have the same number of nearest neighbors as on the actual (100) surface. In the starting geometry of the optimization procedure, acrylonitrile is located above the two central atoms (colored in dark in Fig. 1). Larger clusters having the same two central atoms are also used: $\text{Cu}_{16}(8,8)$, $\text{Cu}_{18}(9,9)$, and $\text{Cu}_{20}(10,10)$.

Geskin *et al.*^{8(e)} suggested that the copper atoms of the cluster that have the lowest spin density are more appropriate to represent the interaction of the metal with an adsorbate. This criterion is based on the nonmagnetic nature of bulk copper, where, intuitively, each bulk atom has no unpaired electrons due to band formation (spin pairing). The spin on surface atoms might be higher, since they are fewer neighbors with which to share the electrons. However, it is expected that even the surface atoms in a nonmagnetic metal present the lowest possible spin. This argument has been used for $\text{Cu}_9(5,4)$, in which the central atom has the same coordination number as on the real (100) surface: only negligible nonzero spin and charge have been calculated on that site. In all the clusters having nonzero spin studied here, the spin density is mostly concentrated on the peripheral Cu at-

TABLE I. Selected structural parameters calculated at the LSD level for the $[\text{Cu}_n\text{-AN}]$ complexes with $n=9\text{--}20$.

Complexes	Bond lengths (Å)							Angle (°)	Eb (kcal/mol)
	C ¹ C ²	C ² C ³	C ³ N	C ¹ Cu	C ² Cu	C ³ Cu	NCu	C ² C ³ N	
AN	1.336	1.410	1.169	180	...
[AN-Cu ₉]	1.427	1.362	1.201	2.08	2.49	2.37	1.89	163	-29.0
[AN-Cu ₁₀]	1.434	1.365	1.204	2.10	2.47	2.36	1.90	173	-32.5
[AN-Cu ₁₁]	1.417	1.373	1.196	2.15	2.56	2.47	1.95	166	-28.9
[AN-Cu ₁₂]	1.404	1.392	1.191	2.12	2.09	2.26	2.11	173	-26.9
[AN-Cu ₁₃]	1.416	1.370	1.195	2.14	2.59	2.49	1.97	167	-24.9
[AN-Cu ₁₄]	1.437	1.362	1.202	2.12	2.62	2.47	1.94	167	-28.6
[AN-Cu ₁₆]	1.435	1.387	1.192	2.14	2.32	2.45	2.20	169	-27.6
[AN-Cu ₁₈]	1.410	1.378	1.196	2.16	2.40	2.50	2.08	166	-26.5
[AN-Cu ₂₀]	1.412	1.371	1.198	2.08	2.38	2.42	2.02	168	-27.2
Average value	1.421	1.373	1.197	2.12	2.32	2.42	2.01	168	-28.0

oms of the upper layer, whose coordination number is the lowest in the clusters.⁴ From this observation, the unsaturated peripheral atoms are not expected to represent the copper surface atoms as accurately as the central atoms of the layer. Hence, copper clusters larger than Cu₁₄(8,6) are expected to be more adequate as surface models for studying the adsorption of acrylonitrile, since two well-saturated copper atoms are capable of interacting with the adsorbate.

B. Computational approach

The calculations are performed in the framework of the density functional theory (DFT).^{10,11} This method is a non-empirical approach, alternative to Hartree-Fock-based theories; it presently finds wider applications to chemical problems due to the possibility of including a significant part of electron correlation energy at a relatively low computational cost. We recall that electron correlation is essential for a correct description of transition metal compounds.

All the calculations are performed using the DMOL program¹²⁻¹⁴ with the DNP (double zeta numeric with polarization) basis set. The core orbitals are frozen during the SCF iterations¹⁵ and a "MEDIUM" mesh size is chosen for the calculations.^{12,14} During the geometry optimizations, the calculations are performed within the local spin density approximation (LSD) with the Vosko-Wilk-Nusair exchange-correlation potential.¹⁶ Geometry optimizations are carried out with the eigenvector-following algorithm by Baker;^{17(a)} this algorithm was improved to optimize the geometry in Cartesian coordinates^{17(b)} and to introduce constraints (fixed atoms) in Cartesian coordinates thanks to an efficient Lagrange multiplier algorithm.^{17(c),(d)} The geometry optimizations are unconstrained except for the distances between metal atoms that are kept at the bulk crystal values (a nearest-neighbor distance of 2.551 Å).

When discussing binding energies, basis-set superposition errors (BSSE) should be estimated; an advantage of the DMOL numeric basis sets is their low BSSE values. For transition metal complexes, the BSSE was estimated to be significantly less than 5 kcal/mol.¹⁸ Note that the binding energies calculated at the LSD level are usually overestimated;¹⁹ however, the LSD approximation gives appropriate adsorption geometries.^{1(e)} Since the LSD method is less computa-

tionally demanding than the gradient-corrected approximations, it allows us to consider rather large clusters with all $3d$, $4d$, and $4p$ atomic orbitals of Cu included in the basis set. The charge analysis used in this work comes from the Hirshfeld scheme, which is directly based on the electronic density.^{20,21}

The vibrational frequencies are calculated in the harmonic approximation by diagonalizing the mass-weighted second-derivative matrix composed of the second derivatives of the total energy with respect to the Cartesian coordinates of atoms.²² The second derivatives are computed by finite differences of the first derivatives using two points on both sides of the equilibrium position of the atoms.¹⁴ The calculation of the vibrational frequencies of the complex composed of the Cu₉ copper cluster and the acrylonitrile adsorbate is performed by considering the movements of both the metal atoms and those of acrylonitrile. The vibrational frequency calculation starts from the optimized geometric structures of adsorbed AN on the cluster with the metal atoms fixed. As a consequence, negative vibrational frequencies appear since the metal cluster is not in a minimum of the Born-Oppenheimer potential surface of the complex. The vibrational modes related to these negative frequencies are characterized exclusively by metal atom movements. The calculated vibrational frequencies of acrylonitrile adsorbed on the copper cluster are thus not expected to be significantly influenced by this effect. In any case, it appears more reasonable to take into account the motions of the metal atoms bound to acrylonitrile to describe the cluster/acrylonitrile bond vibrations rather than to fix these copper atoms during the vibrational frequency calculations.

III. RESULTS AND DISCUSSION

A. Geometric structure of AN copper complexes

The adsorption geometries in all the complexes studied in this work (see Table I) are nearly identical and very similar to that in the $[\text{Cu}_9\text{-AN}]$ complex described by Geskin *et al.*^{8(e)} this is clear evidence that the adsorption geometry calculated even with the smallest copper cluster, i.e., Cu₉, is reliable, even if some atoms involved in the interaction with AN do not have the proper number of nearest neighbors with

respect to the actual surface. The geometric structures of the complexes are represented in Fig. 1. The C=C and the C≡N groups are asymmetrically coordinated to one copper atom. In all complexes, only two copper atoms (colored in dark in Fig. 1) show distances with AN atoms indicating the formation of chemical bonds; the shortest contacts are with the two terminal backbone atoms (C and N): the distance averaged over all the complexes between C¹ and the central copper atom is 2.12 Å and it is 1.99 Å between the nitrogen atom and the closest copper atom; the average distances with the other two carbon atoms are 2.48 and 2.40 Å. The complexes can therefore be considered as di-σ complexes. The binding energy is calculated to be on the order of -28 kcal/mol.

The major changes in bond lengths for AN in the complexes, relative to the isolated molecule, are significant elongations of the C¹-C² and C³-N bonds, while C²-C³ assumes a double-bond character. The reason for this geometric rearrangement is related to the lower availability of the 2*p* electrons of the C and N terminal atoms for the π system, because of their involvement in bonding with copper, and a new π bond is formed between the two central carbon atoms. As a result, the C²C³N bond angle deviates from 180°, which can be interpreted as a change in apparent hybridization of all backbone atoms. Another feature indicating the change in hybridization, from *sp*² to *sp*³, of the C¹ atom is the positions of the adjacent hydrogen atoms that shift away from the plane of the molecule.

The use of complexes composed of an adsorbate interacting with small transition metal clusters, studied at the LSD level of DFT, was shown to give reliable estimates of the experimental vibrational frequencies for the corresponding adsorbate-metal surface systems.²³⁻²⁵ On the basis of this argument and since the adsorption geometry of AN does not change with cluster size, the smallest complex, [Cu₉-AN], is chosen to estimate the vibrational properties of acrylonitrile adsorbed on copper in order to compare with experimental results.²⁶ Upon chemisorption, we expect that the appearance of new bonds translates into new features in the vibrational frequency spectrum and modifications of the features related to isolated AN.

The calculated vibrational spectrum of free acrylonitrile [Fig. 2(a)] indicates that the 15 vibrational modes of AN are active in IR spectroscopy. Table II compares the calculated vibrational frequencies with the experimental data obtained by means of IR and Raman spectroscopy.²⁷ Most of the calculated stretching, rocking, and wagging frequencies are very well evaluated, compared to the experimental data (with errors below 4%). However, we note an important difference between the calculated stretching frequency of the C-C single bond (698 cm⁻¹) and the measured value (869 cm⁻¹); this large difference is partially related to the use of the LSD approximation. Indeed, this vibrational frequency calculated at the gradient-corrected (GC) level of DFT (with the exchange potential by Becke²⁸ and the correlation potential by Perdew and Wang²⁹) is 787 cm⁻¹. The LSD and the GC vibrational frequencies are compared in Table II. We can observe that the difference in exchange-correlation potential significantly affects only the C-C single bond and the C≡N

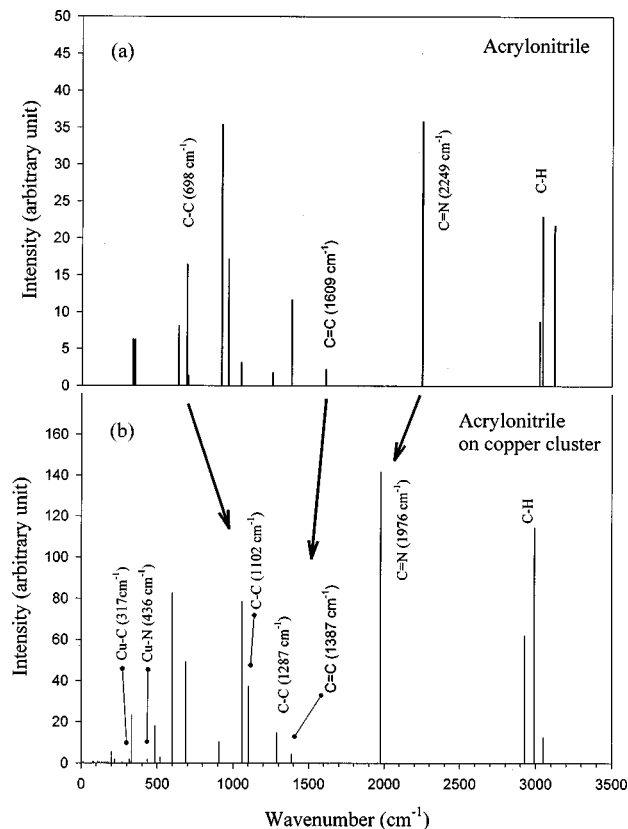


FIG. 2. A comparison between the calculated infrared vibrational frequencies of (a) isolated acrylonitrile; and (b) acrylonitrile interacting with a copper cluster in the [Cu₉(5,4)-AN] complex.

stretching frequencies. Two other frequencies related to the bending of the C-C≡N backbone are also rather poorly evaluated. Since we aim at studying the trends in the modifications of the vibrational properties of AN upon chemisorption on the metal surface, and comparing those trends to experimental measurements, we focus on the frequencies of the stretching modes of the C=C (1609 cm⁻¹, 0.4% error) and C≡N (2249 cm⁻¹, 0.4% error) bonds. These modes are most interesting since they correspond to the unsaturated chemical groups interacting chemically with the metal surface, as described above (Fig. 1).

Figure 2(b) represents the calculated IR spectrum of the [Cu₉-AN] complex, which will be compared to the surface-enhanced Raman (SER) spectrum of the AN copper interface obtained by Loo and Kato.²⁶ Since the experimental spectrum is expected to be influenced by the vibrational Stark effect (resulting from the electric field due to electrode polarization and the medium effect) and the polycrystalline nature of the metal, the comparison with the calculated values can only be semiquantitative.

In the calculated spectrum of the complex [Fig. 2(b)], the low-frequency region (under 300 cm⁻¹) is mainly related to vibration modes of the copper cluster. The frequencies of these vibrations are in good agreement with experimental data obtained for Cu₃, where they are found between 149 and 252 cm⁻¹.³⁰ The adsorption of AN on the copper cluster manifests in the spectrum by new features due to (i) new bonds formed upon chemisorption; and (ii) changes in the

TABLE II. A comparison between the calculated and the measured vibrational frequencies of acrylonitrile.

Harmonic vibrational modes	Raman frequency AN in liquid phase (cm ⁻¹) (Ref. 27)	IR frequency AN in gas phase (cm ⁻¹) (Ref. 27)	Calculated vibrational frequency at LSD level (cm ⁻¹)	Error LSD/exp (cm ⁻¹) vs ν^*	Error LSD/exp (%)	Calculated vibrational frequency at GC level (cm ⁻¹)
C \equiv C \equiv N bend	242*	...	336	94	28	332
C \equiv C \equiv N bend	362*	...	350	-12	3.4	354
C=C-C bend	570*	...	636	66	10.4	651
C=C torsion	688	683*	691	8	1.2	691
C-C stretch	871	869*	698	-175	25	787
H ₂ C=C wag		954*	920	-34	3.7	939
RHC=C wag	970	972*	965	-7	0.7	973
CH ₂ rock	1094	1096*	1050	-46	4.4	1007
C-H rock	1286	1282*	1258	-24	1.9	1225
CH ₂ bend	1412	1416*	1384	-32	2.3	1413
C=C stretch	1607	1615*	1609	-6	0.4	1639
C \equiv N stretch	2228	2239*	2249	10	0.4	2149
C-H stretch	3032	3042*	3022	-20	0.7	3035
C-H stretch	3068	3078*	3042	-36	1.2	3046
C-H stretch	3116	3125*	3119	-6	0.2	3128

backbone. In the experimental spectrum of Ref. 26, a broad peak at 446 cm⁻¹ was assigned to AN-Cu bonds, while no useful information could be obtained below 400 cm⁻¹. In that frequency range, the calculated spectrum shows two peaks (at 220 and 317 cm⁻¹) that are characteristic of the Cu-C stretching (the first mode involves not only the Cu-C stretching but other atomic displacements as well), while the peak at 436 cm⁻¹ represents the stretching of the Cu-N bond. The calculated stretching frequencies are consistent with the results of other experimental studies showing that Cu-N and Cu-C stretchings appear in that frequency range: the Cu-C stretching frequency has been evaluated to be 439 cm⁻¹ in the Cu-CO system,³¹ the Cu-N stretching frequency is 354 cm⁻¹ in the Cu(111)-NO system,³² 315 cm⁻¹ in the Cu(NH₃) complex,²⁵ and 324 cm⁻¹ for Cu(100)-N.³³ Note also that the calculated intensities of the Cu-C and Cu-N stretching modes are small, as found in other theoretical studies.^{25,31}

Different adsorption geometries of AN on a polycrystalline copper electrode could be considered: for instance, di- σ adsorption via the two terminal atoms (C and N) [Fig. 1 and Fig. 3(a)]; di- π adsorption via the C=C and C \equiv N groups [Fig. 3(b)]; di- σ adsorption as proposed by Loo and Kato [Fig. 3(c)] that occurs via the two atoms of the nitrile group and differs from the di- σ adsorption optimized here; or end-on σ adsorption via the lone pair electrons on the N atom [Fig. 3(d)]. From our calculations, we have found that the complex where acrylonitrile is bound end on to the central atom of Cu₉ is less stable (Eb = -8.6 kcal/mol) than the optimal di- σ adsorption complex (Eb = -29.0 kcal/mol, Fig. 1). As a consequence, we expect that this end-on adsorption geometry is not the dominant adsorbed species on the copper electrode at its potential of zero charge (PZC) or at the cathodic polarization used in the electrografting experiment. However, note that (i) an acrylonitrile molecule positioned perpendicular to the surface has a C \equiv N stretching intensity higher than the C=C stretching intensity of acrylonitrile flat adsorbed on a metal surface; hence, within the same vibrational spectrum, the intensities of the peaks corresponding to

different species are not easily related to the concentrations. (ii) End-on adsorption of acrylonitrile could occur if the electrode is anodically polarized due to the favorable orientation of its dipolar moment along the electric field present at the vicinity of the anode. (iii) Since the experimental spectrum is related to acrylonitrile at the vicinity of a polycrystalline copper surface and since the AN adsorption geometry is expected to be different depending on the Miller indices of the sections of the copper surface and surface defects, the experimental spectrum is likely made of a superposition of vibrational frequencies of different adsorption geometries of acrylonitrile.

The stretching frequencies of the bonds along the AN backbone are strongly modified upon chemisorption.

(i) The calculated spectrum indicates that the C=C double bond frequency evolves from 1609 to 1387 cm⁻¹; this is due to the increase in C¹=C² bond length in all complexes [Cu_n(y,w)-AN] (from 1.34 to 1.42 Å; see Table I, since the terminal carbon atom (C¹) interacts with one copper atom via the 2p π atomic orbital to form a σ bond [Fig.

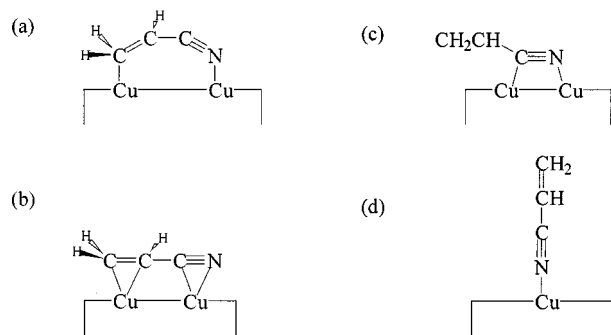


FIG. 3. Different proposals for the adsorption geometry of acrylonitrile on a polycrystalline copper surface: (a) the di- σ adsorption via the two terminal atoms (C and N); (b) the di- π adsorption via the C=C and C \equiv N group; (c) the di- σ adsorption proposed by Loo *et al.*, which occurs via the two atoms of the nitrile group; and (d) the end-on σ adsorption via the lone pair electrons on the N atom.

3(a)]. In relation to their experimental spectrum, Loo and Kato also mention a significant decrease in C=C stretch due to the chemisorption of AN parallel to the surface. However, the experimental observation can actually be related to either the di- π adsorption suggested by Loo and Kato [i.e., both carbon atoms would be involved in the interaction with one copper atom; see Fig. 3(b)] or the di- σ adsorption calculated here [Fig. 1 and Fig. 3(a)]. Note that Loo and Kato proposed that the experimental peak at 1603 cm^{-1} , very similar to that of free AN, is related to the C=C stretch of AN bound end-on to the Cu surface through the lone pair electrons of the nitrile group [Fig. 3(d)].

(ii) The involvement of the nitrile group in the chemisorption with the copper clusters is shown to induce significant elongation in the C≡N bond (from 1.17 to 1.20 Å; see Table I). This modification leads to a strong decrease in C≡N stretching frequency upon chemisorption, from 2249 to 1976 cm^{-1} . The most intense band in the SER spectrum is located at 2082 cm^{-1} ; it was assigned to the stretching of the C≡N group π bonded to the copper surface [Fig. 3(b)]. Loo and Kato tentatively assigned the 1972 cm^{-1} band in the experimental spectrum to the same stretching mode (C≡N group π bonded), but for AN adsorbed on a different site of the surface. Note the correspondence between the latter peak (1972 cm^{-1}) and the calculated frequency (1976 cm^{-1}) related to C≡N stretching in our model, in which within the C≡N bond only the nitrogen atom interacts with a copper atom, via the $2p\pi$ atomic orbital, to form a σ bond [Fig. 3(a)].

(iii) As mentioned above, the formation of a di- σ adsorption via the two terminal atoms (C¹ and N) of the AN backbone increases the C=C and C≡N bond lengths, and shortens the C²-C³ bond (from 1.41 to 1.37 Å), i.e., increases its double bond character. As expected, the frequency of the C²-C³ bond stretching increases upon chemisorption: from 698 cm^{-1} to 1102 and 1287 cm^{-1} (these modes involve not only the C-C stretch but also other atomic motions), in contrast to the C=C and C≡N stretching.

We believe that the di- σ adsorption described in Fig. 1 [which differs from the di- σ proposed by Loo and Kato; see Fig. 3(c)], is the most probable adsorption configuration of AN on the Cu(100) surface. The di- σ adsorption configuration proposed by Loo and Kato should more likely occur on surfaces more compact than Cu(100). The semiquantitative agreement between the experimental SER spectrum and the calculated vibrational spectrum of acrylonitrile di- σ adsorbed on Cu(100) indicates that the acrylonitrile monomer is chemisorbed parallel to the polycrystalline copper electrode at its PZC or at low cathodic polarization. Hence, AN chemisorbed as described in this study can be considered a good model for the actual initial step of the electroreduction of chemisorbed acrylonitrile.

B. Charge transfer upon chemisorption

Chemisorption leads to partial electron transfer between the copper cluster and the AN molecule. This appears in the calculated Hirshfeld charge distribution, which shows a partial negative charge ($\cong -0.28|e|$) located on AN and a partial positive charge on the copper cluster. This charge trans-

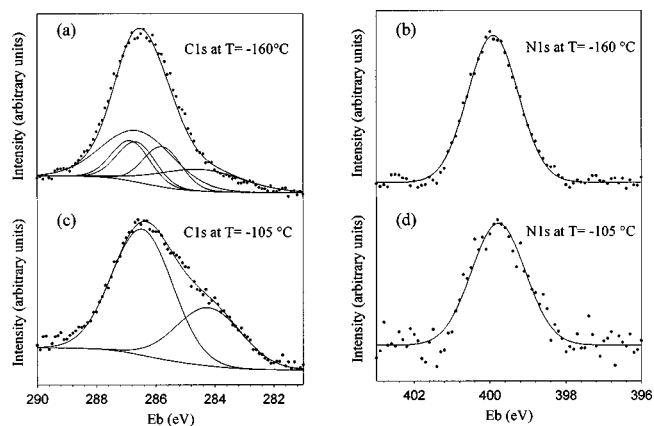


FIG. 4. XPS C 1s (a) peak and N 1s peak (b) of a multilayer of acrylonitrile adsorbed on the copper surface at $T = -160^\circ\text{C}$. XPS C 1s peak (c), and N 1s peak (d) of acrylonitrile remaining after evaporation of the multilayer at $T = -105^\circ\text{C}$. Binding energies (Eb) of the core electrons are given in eV.

fer and the strong geometric changes in AN upon adsorption are clear evidence of the chemical nature of the interaction. The rearrangement of the electronic density in the AN/Cu system can be characterized by means of XPS; here, we present the most relevant XPS data on the AN/Cu adsorption.

The copper surface used for the XPS measurements conducted in Linköping is obtained from a polycrystalline copper surface sputtered in the ultrahigh vacuum (UHV) preparation chamber of the XPS spectrometer, with neon ions accelerated onto the metal surface by a voltage of 5 kV. After sputtering, the cleaned copper surface is found to be free of carbon contamination and surface oxide. The metal surface is then cooled to -170°C and exposed to acrylonitrile vapor ($P \cong 10^{-7}\text{ Torr}$), in order to form a multilayer of acrylonitrile condensed on the surface. Once the multilayer is formed, the sample is introduced in the UHV analysis chamber of the spectrometer for XPS measurements. In order to avoid surface charging, the thickness of the condensed layer is maintained well below 100 Å; this is carried out by checking the presence of the copper peaks in the XPS spectra.

The acrylonitrile multilayer is characterized by a broad C 1s signal [Fig. 4(a)] at 286.5 eV and a N 1s peak at 399.9 eV [Fig. 4(b)]. The C 1s signal in Fig. 4(a) is difficult to interpret because it is composed of contributions from the three different carbon atoms of nonchemisorbed acrylonitrile in the multilayer, and from the chemisorbed acrylonitrile monolayer. Hence, we rationalize this broad C 1s signal after the characterization of the chemisorbed monolayer. Starting from the acrylonitrile multilayer, the sample is gradually warmed up to exceed the vaporization temperature of AN ($T_{\text{vap}} \cong 145^\circ\text{C}$ for $P = 3 \times 10^{-9}\text{ Torr}$). The effect of the increase of temperature is illustrated in Fig. 5. The C 1s [Fig. 5(a)] and N 1s [Fig. 5(b)] intensities show a sharp decrease around -145°C , while the Cu 2p copper signal [Fig. 5(c)] increases simultaneously. The evolution of the spectra correspond to the evaporation of the acrylonitrile multilayer. Note that during this temperature increase, the C 1s/N 1s ratio is constant, which indicates that no chemical decomposition is taking place on the surface. Above -120°C , the C 1s and

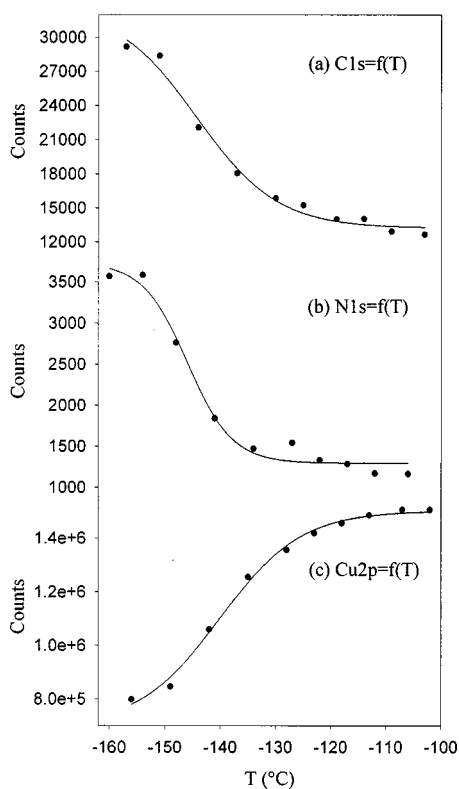


FIG. 5. Evolution of the XPS C 1s (a), N 1s (b), and Cu 2p (c) peak intensities for acrylonitrile adsorbed on a polycrystalline copper surface, with respect to the temperature.

N 1s peak intensities are constant; this corresponds to the chemisorbed acrylonitrile monolayer. This acrylonitrile monolayer is characterized by a broad C 1s signal [Fig. 4(c)] that can be decomposed into two components: the first one at 286.5 eV is approximately twice as intense as the second one, centered at 284.3 eV. The latter is broader and shifted by 2.2 eV to lower binding energy with respect to the center of the multilayer signal. This large shift toward smaller binding energy indicates that the electronic density around some carbon atoms has increased upon chemisorption. This observation is in qualitative agreement with the changes in Hirshfeld atomic charges calculated for the largest model complex $[\text{Cu}_{20}\text{-AN}]$; the atomic charge of the CH_2 carbon atom becomes indeed significantly more negative ($\Delta q = -0.113|e|$); the negative charge on the CH carbon slightly increases ($\Delta q = -0.024|e|$) upon chemisorption, while it decreases weakly on the carbon atom of the nitrile group, $\Delta q = +0.016|e|$. We propose therefore that the C 1s component at the lowest binding energy (284.3 eV) comes from the CH_2 carbon atoms and that the peak at 286.5 eV includes both the CH and $\text{C}\equiv\text{N}$ signals of chemisorbed acrylonitrile. Note that the large width of these two components and the intensity ratio between the two components, which slightly deviates from 2:1, is probably due to the existence of other adsorption geometries of acrylonitrile (such as those presented in Fig. 3) on other faces and sites of the polycrystalline copper surface used in the experiment. Another important feature of AN chemisorption is the absence of shift of the N 1s binding energy upon chemisorption. The N 1s intensity decreases

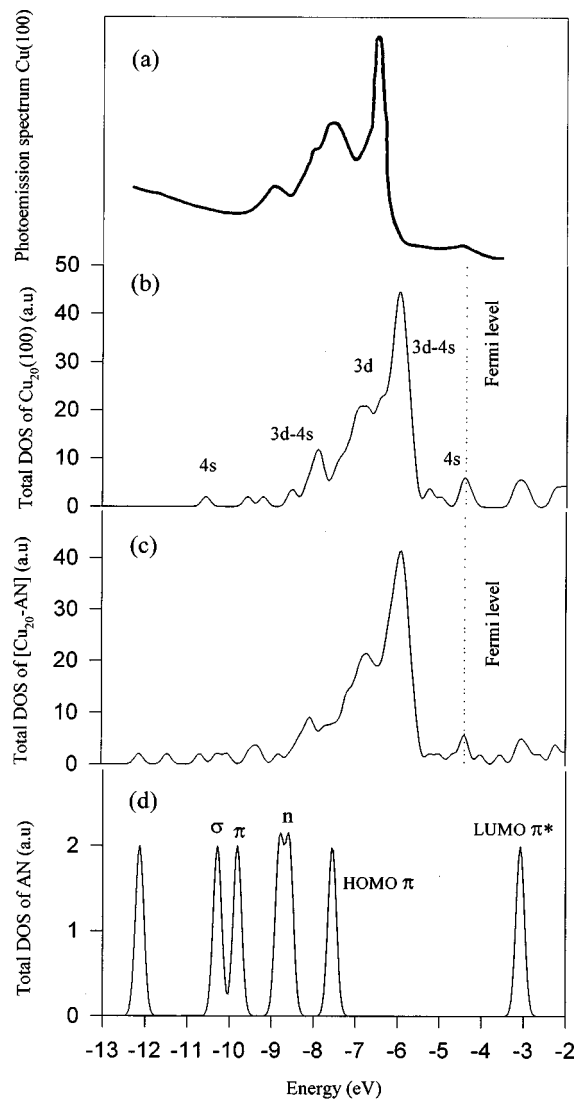


FIG. 6. Photoemission spectrum of the Cu(100) surface (Ref. 39) (a) and total density of states (DOS) of (b) the $\text{Cu}_{20}(10,10)$ cluster; (c) the $[\text{Cu}_{20}(10,10)\text{-AN}]$ complex; and (d) the acrylonitrile molecule.

significantly around the vaporization temperature, but the binding energy evolves only weakly, from 399.9 eV for the multilayer [Fig. 4(b)] to 399.8 eV for the monolayer [Fig. 4(d)], which is within the error bars for the measurement. This is consistent with our theoretical results, which indicate no modification in the atomic charge on the nitrogen atom upon chemisorption, due to a donation-retrodonation mechanism (see Sec. III C).

We are now able to propose an explanation for the broad C 1s peak observed for the acrylonitrile multilayer at -160°C [Fig. 4(a)]. The Cu 2p intensity decreases only by a factor of 1.9 upon evaporation of the multilayer [Fig. 5(a)]. In a first approximation, the logarithm of this factor corresponds to the ratio between the thickness of the condensed AN molecule on the chemisorbed monolayer and the escape depth of the Cu 2p photoelectrons. The multilayer is then probably formed of only two or three layers. Consequently, the chemisorbed monolayer participates significantly in the C 1s signal of the multilayer [Fig. 4(a)]. We then locate two broad components at 286.5 and 284.3 eV with an intensity

ratio close to 2, as observed in the monolayer [Fig. 4(c)]. We then add one component for each of the three carbon atoms of acrylonitrile in nonchemisorbed layers of the multilayer. The width of these three components is taken as the typical width of a C 1s peak (1.5 eV) measured with our spectrometer, and their intensity are set to be identical. The binding energy differences between these three components is kept equal to those obtained in XPS experimental studies of gas phase acrylonitrile^{34(a)} and theoretical evaluations of the core–electron binding energies obtained by Bureau *et al.* with the Generalization of the Slater Transition State method used in DFT.^{34(b)} Although a real deconvolution is not possible for the broad C 1s peak, the sum of the three components at 285.77, 286.65, and 286.84 eV attributed to the CH₂, CH, and CN carbon atoms of the nonchemisorbed layers of the multilayer, respectively; and the two broad components at 286.5 and 284.3 eV corresponding to the chemisorbed monolayer, is in good agreement with the experimental spectrum [Fig. 4(a)].

The partial charge transfer from the metal to acrylonitrile can be understood on the basis of the chemical potentials of the two compounds. When the two components come into interaction, their electronic chemical potentials tend to equalize; this determines the direction of electron transfer,^{35(a),(b)} from the species with the higher chemical potential toward

that with the lower chemical potential. The electronic chemical potential μ and chemical hardness η of AN can be estimated from its vertical ionization potential IP and electron affinity EA values:^{35(c)}

$$\mu = -\frac{\text{IP} + \text{EA}}{2} \quad \text{and} \quad \eta = \frac{\text{IP} - \text{EA}}{2}. \quad (1)$$

Here, $\text{IP} = E^+ - E^0$ and $\text{EA} = E^0 - E^-$, with E^+, E^0, E^- being the total energies of the cationic, neutral, and anionic species in the equilibrium geometry of the neutral species. For AN, we obtain $\text{IP} = 11.00$ eV and $\text{EA} = -0.03$ eV, thus $\mu_{\text{AN}}^0 = -5.49$ eV (and $\eta_{\text{AN}}^0 = 5.51$ eV). Whatever the size of the copper clusters used in this work, the chemical potentials are very similar, in a range between -4.11 and -4.36 eV; these values are very close to that of an actual copper surface (-4.65 eV), as obtained in a recent work.⁴ Therefore, electronic charge transfer is expected to occur from the copper clusters or the actual copper surface (the Lewis base) toward AN (the Lewis acid); the same situation is found for methacrylonitrile adsorbed on nickel.^{8(c)}

When reactants approach, the external potential felt by their electrons changes and there is a flow of electrons ΔN that allows the chemical potential equalization. ΔN is inversely proportional to the sum of the hardness of the reactants;^{10,35(a)} for AN and Cu_{*n*},

$$\Delta N = \frac{(\mu_{\text{AN}}^0 - \mu_{\text{Cu}_n}^0) + \int f_{\text{AN}}^+(r) \Delta v_{\text{AN}}(r) dr - \int f_{\text{Cu}_n}^-(r) \Delta v_{\text{Cu}_n}(r) dr}{2(\eta_{\text{AN}} + \eta_{\text{Cu}_n})}, \quad (2)$$

where $\mu_{\text{Cu}_n}^0$, μ_{AN}^0 and η_{Cu_n} , η_{AN} are the chemical potential and hardness of the isolated reactants; $f_{\text{AN}}^+(r)$ and $f_{\text{Cu}_n}^-(r)$ are the Fukui functions^{35(d),(e)} of AN (which gains a partial electron charge) and the copper cluster (which loses partial charge); Δv_{AN} is the variation of the external potential felt by the electron cloud of AN due to the approach toward the copper cluster. Three parameters of the numerator are susceptible to change with cluster size: $\mu_{\text{Cu}_n}^0$, Δv_{AN} , and $f_{\text{Cu}_n}^-(r)$; however, the chemical potential of the clusters $\mu_{\text{Cu}_n}^0$ has been shown to be nearly constant with size⁴ while the other two terms in the numerator nearly cancel, and their difference is not expected to change significantly with size since chemisorption is mainly a local phenomenon.³⁶ Hence, as the numerator is expected to be quasicontant with cluster size, the variation in hardness of the copper clusters, appearing in the denominator, leads to the size dependence of the charge transfer upon chemisorption. A significant decrease in hardness of copper clusters with increasing size has been calculated previously;⁴ therefore, the charge transfer is expected to be larger between the actual Cu(100) surface and AN than between small copper clusters and AN.

As the hardness of copper clusters decreases with size, the hard–soft character of the interaction with AN increases. As a consequence, the chemisorption energy cannot be associated exclusively with charge transfer stabilization (impor-

tant in soft–soft interactions^{35(a)} or exclusively with external potential perturbation (important in hard–hard interactions^{35(a)}). Instead, both contributions are important, which makes the estimate of the chemisorption energy from the global properties rather delicate. Moreover, the transferred charge, the chemical potential, and the bond hardness are well known to evolve along the reaction path,³⁷ which emphasizes the fact that only qualitative information can be obtained from such global properties. To have more insight into the molecular orbital rearrangements due to chemisorption and leading to partial charge transfer, an analysis of the molecular orbitals of the adsorbed species can be helpful.

C. Chemisorption as mixing of molecular orbitals

Chemisorption can be characterized in terms of interaction between the molecular orbitals (MOs) of AN and those of the copper clusters. The complex studied for this purpose is [Cu₂₀(10,10)–AN] since the density of states (DOS) of Cu₂₀(10,10) is very similar to that in the experimental photoemission spectrum of Cu(100),^{38,39} see Fig. 6. Figure 6 also displays a comparison between the total DOS of the [Cu₂₀–AN] complex and the total DOS of the two isolated partners. The appearance of new peaks in the total DOS of

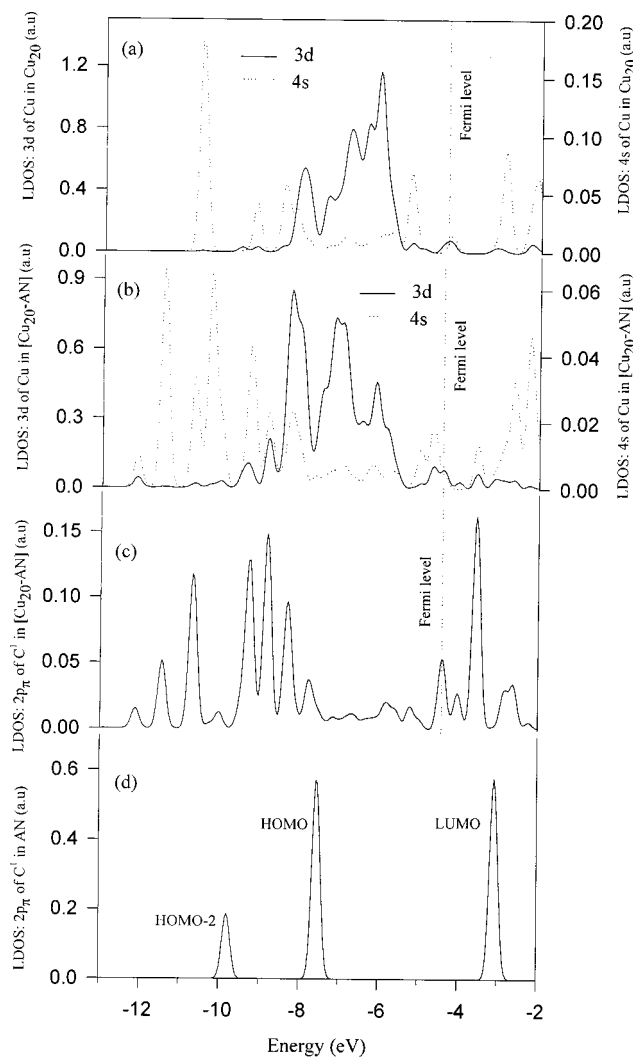


FIG. 7. Evolution of the Local Density of States [LDOS, following the decomposition scheme by Löwdin (Ref. 40)] upon the formation of the Cu–C bond between acrylonitrile and the copper cluster: (a) LDOS (projected on the $3d$ and $4s$ atomic orbitals) of the isolated copper cluster located on the copper atom interacting with the carbon atom of acrylonitrile in the $[\text{Cu}_{20}(10,10)\text{-AN}]$ complex; (b) LDOS (projected on the $3d$ and $4s$ atomic orbitals) of the $[\text{Cu}_{20}(10,10)\text{-AN}]$ complex located on the copper atom interacting with the carbon atom of acrylonitrile; (c) LDOS of the $[\text{Cu}_{20}(10,10)\text{-AN}]$ complex located on the carbon atom of acrylonitrile interacting with the copper cluster; and (d) LDOS of acrylonitrile located on the carbon atom of acrylonitrile interacting with the copper cluster.

the complex with respect to that of the copper cluster is observed among occupied levels as well as unoccupied levels.

The $[\text{Cu}_{20}\text{-AN}]$ interaction can be analyzed in terms of the local DOS (Figs. 7 and 8), following the decomposition scheme by Löwdin.⁴⁰ Since our aim is to describe the dominant chemisorption mechanism and we expect that AN lies rather flat on the surface of Cu_{20} and is chemisorbed by means of its two terminal backbone atoms (C, N), the relevant orbital overlaps are those between the π orbitals ($2p\pi$ orbitals pointing perpendicularly to the metal surface) of AN and the $4s, 3d$ levels of Cu_{20} . Hence, the fact that we consider only the LUMO, HOMO, and HOMO-2 of AN (MOs composed of $2p\pi$ orbitals) in the description of the interaction between AN and Cu(100) is not related to frontier orbit-

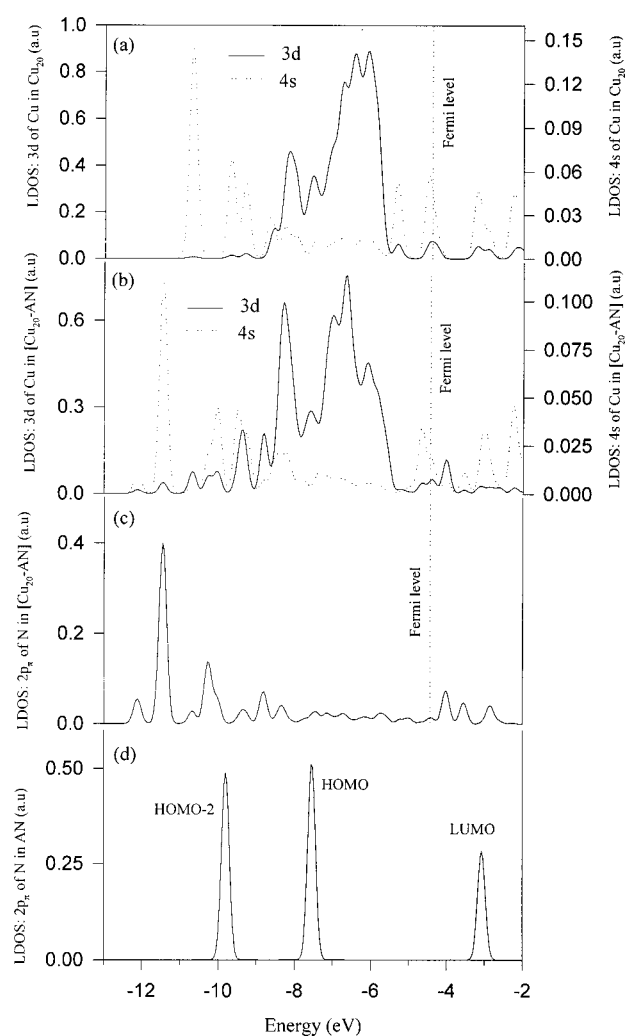


FIG. 8. Evolution of the Local Density of States [LDOS, following the decomposition scheme by Löwdin (Ref. 40)] upon formation of the Cu–N bond between acrylonitrile and the copper cluster: (a) LDOS (projected on the $3d$ and $4s$ atomic orbitals) of the isolated copper cluster located on the copper atom interacting with the nitrogen atom of acrylonitrile in the $[\text{Cu}_{20}(10,10)\text{-AN}]$ complex; (b) LDOS (projected on the $3d$ and $4s$ atomic orbitals) of the $[\text{Cu}_{20}(10,10)\text{-AN}]$ complex located on the copper atom interacting with the nitrogen atom of acrylonitrile; (c) LDOS of the $[\text{Cu}_{20}(10,10)\text{-AN}]$ complex located on the nitrogen atom of acrylonitrile interacting with the copper cluster; and (d) LDOS of acrylonitrile located on the nitrogen atom of acrylonitrile interacting with the copper cluster.

als arguments, but rather to this geometrical argument. First, the interaction between the carbon atom of AN and the copper atom of Cu_{20} involved in the C–Cu bond is analyzed using the local densities of states (Fig. 7). Figures 7(a) and 7(b) represent the molecular orbitals of the Cu_{20} cluster and those of the complex, including the $3d$ (straight line) and $4s$ (dotted line) atomic orbitals (AO) of the copper atom, which is involved in the Cu–C interaction in the complex. The difference between Figs. 7(a) and 7(b) is the result of (i) the mixing between the molecular orbitals of Cu_{20} and those of AN; and (ii) the new potential felt by the $3d$ and $4s$ Cu electrons due to the presence of the acrylonitrile molecule. Figures 7(d) and 7(c) are related to the MOs of isolated AN and those of the complex, highlighting the $2p\pi$ AO of the carbon involved in the Cu–C bond in the complex. The

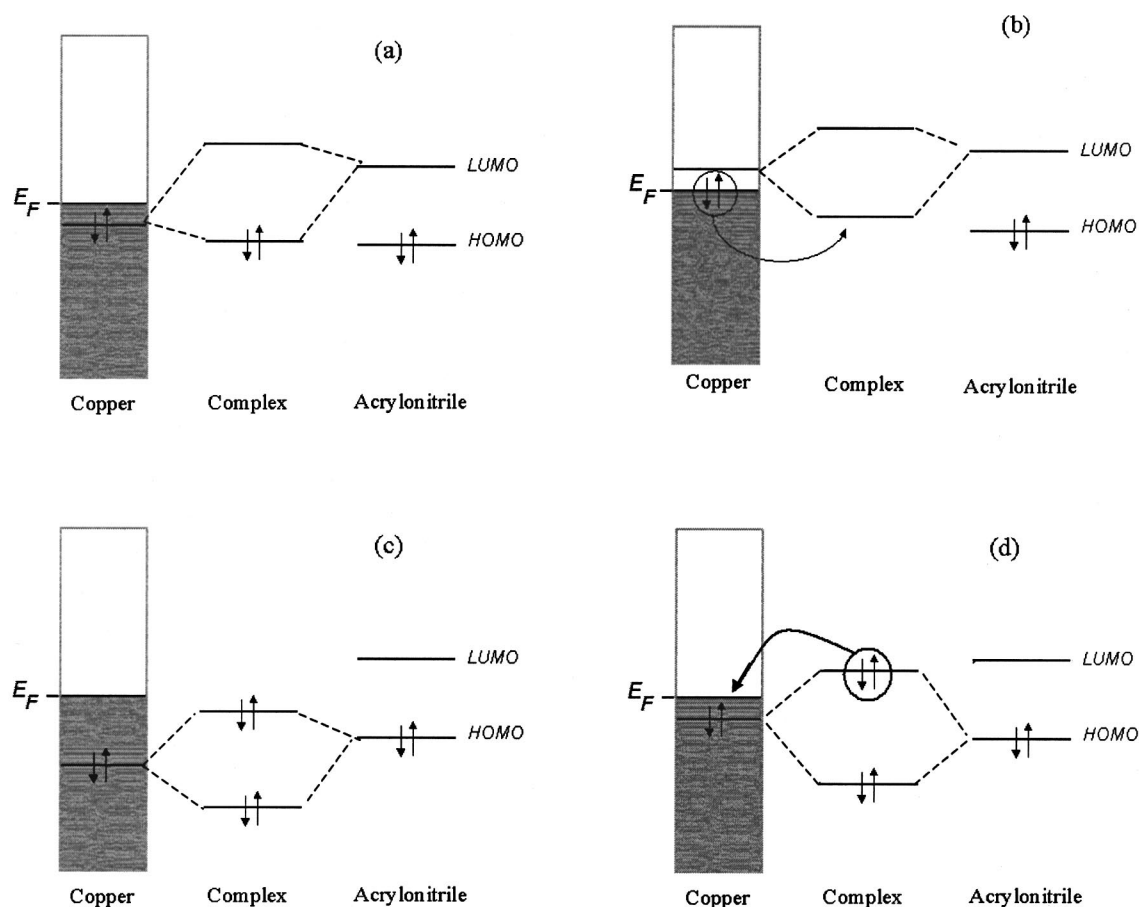


FIG. 9. Schematic illustration of possible molecular orbital mixings between the MOs of acrylonitrile and those of the copper surface upon chemisorption.

bonding (and antibonding) interactions between the AOs of AN and those of Cu_{20} are confirmed by the presence of MOs (peaks in the local DOS) of the complex, which contain both the $2p\pi$ AO of the carbon atom [Fig. 7(c)] and the $3d$ or $4s$ AOs of the copper atom [Fig. 7(b)], for instance, the band located at the ‘‘Fermi level’’ of the complex.

Since the photoemission spectrum of $\text{Cu}(100)$ is very similar to the calculated DOS of Cu_{20} , it seems reasonable to deduce the mechanisms involved in the chemisorption of AN on $\text{Cu}(100)$ from the analysis of the local DOS of $[\text{Cu}_{20}\text{-AN}]$. In isolated AN [Fig. 7(d)], the peak at -3 eV corresponds to the LUMO level. Upon adsorption, this peak is split into different MOs [Fig. 7(c)]; some of them can become occupied, which gives rise to a charge transfer from the cluster to AN. The contribution of the LUMO of AN to the highest occupied MOs of the complex could be due to two mechanisms:⁴¹ (i) the interaction between the LUMO of AN and the $4s-3d$ occupied states of the cluster located just below the Fermi level [Fig. 9(a)]; and (ii) the interaction between the LUMO of AN and the lowest unoccupied MOs of the cluster, generating MOs just below the Fermi level of the complex (because of the small gap in the cluster); this kind of MO becomes consequently occupied by an electron of the metal [Fig. 9(b)]. The interaction between the LUMO of AN and the $3d-4s$ or $4s$ levels is indeed present, as indicated by the correspondence between the peaks in the (-3 to -5 eV) energy range in Figs. 7(b) and 7(c). These interactions stabi-

lize the complex and give rise to a charge transfer from the copper cluster toward AN.

The peak related to the HOMO level of AN [-7.5 eV in Fig. 2(d)] also splits into several peaks upon chemisorption [Fig. 7(c)]. The interaction between the HOMO of AN and the inner occupied states of Cu_{20} , is a two-orbital, four-electron interaction that destabilizes the complex [Fig. 9(c)]. This kind of interaction is likely responsible for the changes in the shape of the local DOS of the $3d$ states on the interacting copper atom [a comparison between Figs. 7(a) and 7(b)]. Furthermore, it is important to notice that the interaction between the HOMO level of AN and the uppermost $4s-3d$ occupied levels of Cu_{20} could formally give rise to doubly occupied antibonding MOs above the Fermi level of the complex [Fig. 9(d)]. That situation would spontaneously stabilize by depopulation of that antibonding level in favor of a lower unoccupied MO of the complex, as explained by *te Velde et al.*⁴² in their study of the CO chemisorption on copper. This stabilization mechanism is possible because of the proximity between the MOs in the complex and the small electronic gap of the complex (0.05 eV). Note that this type of stabilization is most effective for a metal, since in that case the electrons that were in the antibonding level end up at the Fermi level. The peak at -10 eV in the local DOS of isolated AN [Fig. 7(d)] is related to the HOMO-2 of AN. This peak also splits into smaller peaks of lower energy [a comparison between Figs. 7(d) and 7(c)], mostly due to the

interaction with the $4s$ occupied states [a comparison between Figs. 7(c) and 7(b)]. Since the MOs of the complex formed by this interaction are of low energy, they are probably all occupied; this globally corresponds to a destabilization process.

A similar analysis is performed for the Cu–N bond, on the basis of the local DOS represented in Fig. 8. The first two graphs, Figs. 8(a) and 8(b), are related to the copper atom involved in the Cu–N bond, while Figs. 8(c) and 8(d) are local DOS for the nitrogen atom. The local DOS in isolated AN [Fig. 8(d)] is similar to that observed for the carbon atom [Fig. 7(d)]. This means that the $2p\pi$ AO of both the carbon and nitrogen atoms are involved in the LUMO, HOMO, and HOMO-2 of AN. The analysis of the local DOS reveals the same kind of interactions as for the Cu–C bond (Fig. 9): the LUMO, HOMO, and HOMO-2 levels of AN containing the $2p\pi$ AO of nitrogen split into several peaks and spread over a broad range of energy (a comparison between Figs. 8(d) and 8(c)). The correspondence in energy between the peaks in Fig. 8(b) and those in Fig. 8(c) shows the presence of various possible interactions, as proposed for the Cu–C bond: (i) the interaction between the LUMO of AN and either the filled $3d$ or $4s$ states of Cu_{20} (charge transfer) [Fig. 9(a)] or the empty $3d$ or $4s$ states of Cu_{20} , to produce new levels below the Fermi level of the complex, which stabilizes the complex [Fig. 9(b)]; (ii) the interaction between the HOMO of AN and either the inner occupied $3d$ or $4s$ levels of Cu_{20} (repulsive interaction) [Fig. 9(c)], or the uppermost occupied $3d$ or $4s$ levels of Cu_{20} , to produce antibonding levels that are empty because they are located above the Fermi level of the complex [Fig. 9(d)]; (iii) destabilizing interaction following the mixing between the HOMO-2 level of AN and the $3d$ and $4s$ states of Cu_{20} .

Note that the invariant atomic charge of the nitrogen atom upon chemisorption is explained by partial donation of an electron to AN due to molecular orbital mixing between the LUMO of AN and filled [Fig. 9(a)] or empty [Fig. 9(b)] MOs of the metal; accompanied by partial donation of electron to the metal (retrodonation from AN) via the HOMO of AN and filled MOs of the metal [Figs. 9(c) and 9(d)] (the contribution of the mixing between the empty MOs of the metal and the HOMO of AN should be small, since the HOMO is energetically far from the Fermi level of the metal). This theoretical explanation is in agreement with the constant binding energy of the N $1s$ photoelectrons found for the multilayer and the chemisorbed acrylonitrile monolayer in the XPS measurements discussed in the previous section.

The reorganization of the molecular orbitals of the two constituents, Cu_{20} and AN, following the formation of a stable complex, shows some features: the creation of new bonding interactions between AN and Cu_{20} is accompanied by the appearance of less bonding interactions within AN, related to the elongation of the C=C double bond and C≡N triple bond. In addition, we expect modifications in the Cu–Cu bonds of the clusters; which would lead to surface reconstruction upon chemisorption. Note that since the positions of the copper atoms have been fixed, the stabilizing effect of the reconstruction is not considered here. Despite the fact that we neglect this stabilizing effect, AN is found to

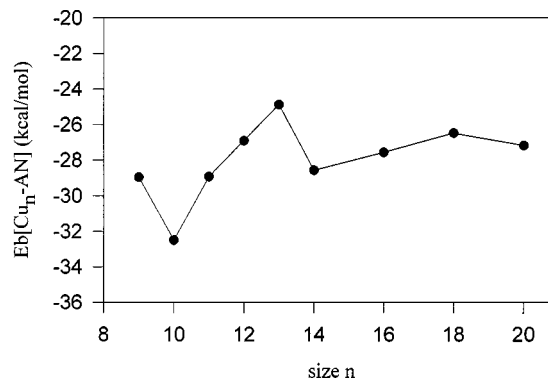


FIG. 10. Evolution of the LSD binding energy (E_b) of acrylonitrile chemisorbed on copper clusters Cu_n of increasing size ($n=9-20$). The binding energy is defined as the difference between the total energy of the $[\text{Cu}_n\text{-AN}]$ complex and the sum of the total energies of the two isolated parts Cu_n and AN.

be chemisorbed on copper clusters, which emphasizes the strong ability of copper to interact with AN. The energies of chemisorption obtained here are thus the result of the competition between stabilizing mechanisms and destabilizing interactions described above.

D. Chemisorption energy versus cluster size

Numerous studies have shown that the binding energy of an adsorbate interacting with metal clusters oscillate with cluster size. The magnitude of these oscillations reaches 20 kcal/mol for CO on Cu_n clusters,^{42,43} 40 kcal/mol for H on W_n ,⁴⁴ and 40 kcal/mol for CO on Ni_n .⁴⁵ The origin of the oscillation comes from the electronic configuration of the metal clusters:²¹ the energy distribution of the one-electron levels is discrete and can dramatically change with the size or shape (symmetry) of the cluster. Some clusters have a favorable electronic configuration and give rise to strong chemisorption. In other words, a given adsorption site possesses an adequate electronic configuration if the symmetry of the molecular orbitals of the adsorbate involved in the bonding and the symmetry of those present on the adsorption site are similar; the energy difference between the molecular orbitals involved in the bond is also an important parameter.⁴⁶ The main difference between metal clusters and the metal surface is the electronic configuration that is discrete for a cluster and a continuum for a surface. In this simple picture, this continuum of states around the Fermi level strongly increases the probability for the real metal surface to have monoenergetic levels of adequate symmetry and energy to form a bond with the adsorbate.

However, for AN interacting with copper clusters, we find that the evolution of the binding energy with cluster size (Fig. 10) displays a rather weak oscillation with a magnitude of *ca.* 8 kcal/mol. It must be noted that in previous studies treating the size effect,^{2,42-44,47} the adsorbate happened to interact with the clusters via a single site. In our case, acrylonitrile interacts with two moieties: the C=C double bond and the nitrile group C≡N. The presence of two interaction sites for AN on our clusters can be partly responsible for the relative weakness of the oscillation of the chemisorption en-

ergy (intuitively, it might be considered that if the electronic configuration of the cluster is not the most appropriate for interaction with one end of AN, this configuration may be more adequate for interaction with the other end of AN; hence there could exist an average effect). For a large number of bonds between the adsorbate and the cluster, one may therefore expect a stronger damping of the oscillating behavior of the chemisorption energy.

Figure 10 indicates that the chemisorption energy changes most importantly in the range of sizes $n=9-13$, while from $n=14-20$, it becomes nearly constant. The changes found from $n=9$ to 13 could be due to the modification in the saturation of the peripheral copper atom that is directly bound to AN. For sizes larger than 13 atoms, the two copper atoms involved in the chemisorption have the same number of nearest neighbors as a copper atom on an actual Cu(100) surface.

Another effect that could decrease the oscillations is the proximity of the electronic levels in our clusters, which is due to their low symmetry, as explained in a previous work.⁴ The proximity of the electronic levels is related to the polarizability and hardness of the electronic clouds.⁴⁸ The electrons of a metal cluster with high polarizability or small hardness can be redistributed easily and compensate for a situation that would not be ideal for bonding, thus allowing for the stabilizing mechanisms discussed above. This damping effect of the oscillations should be enhanced when the size of the cluster increases, since the chemical hardness decreases⁴ and thus its polarizability increases. Therefore, as suggested by Siegbahn *et al.*,⁴⁹ the electronic density of larger clusters should have increased flexibility than in small clusters to create stronger bonds between the metal clusters and the molecules, an effect which can be partly responsible for the nearly constant chemisorption energy for copper clusters larger than 14 atoms.

Hence, the estimate of the chemisorption energy of AN on Cu(100) that we obtain (Table I), -28 kcal/mol, appears to be reasonable and independent of cluster size effects. Note that, on one hand, this chemisorption energy value is obtained in the LSD approximation of DFT, which is known to overestimate the binding energy. On the other hand, the reconstruction effects of the surface that are expected to further stabilize chemisorption are neglected in our model. These two effects should therefore compensate.

We conclude this section by noting that the importance of the metal polarizability in the chemisorption process can also be discussed more fundamentally. First, Falicov *et al.*⁵⁰ have argued that the catalytic activity of transition metals surfaces is associated to their low-energy density electronic fluctuations, which require the presence of low-energy electronic excitations. Second, Yang *et al.*⁵¹ have shown that the local softness of the metal surface is a probe of the local fluctuations in electronic density. Hence, since the local softness is the product between the Fukui function and the global softness, a small hardness (high softness) indicates a reactive metal and mapping the Fukui functions shows, where, on the surface, reactivity and chemisorption are favored. Third, Vela *et al.* have shown that the polarizability can be ex-

pressed via the hardness and the Fukui function;⁴⁸ thus, a high polarizability could also be a reactivity index.⁵²

E. Entropy and free enthalpy of adsorption

In the previous sections, we were interested in the chemisorption energy of AN on Cu(100), which corresponds to an estimate of the enthalpic modification of the [Cu(100)+AN] system upon adsorption. To estimate the free enthalpy of adsorption, ΔG_{ads} , one must take into account the entropy modification upon chemisorption. When AN is adsorbed onto the metal from the gas phase, the organic molecule, which had translational, rotational, and vibrational freedom, is trapped in a potential well and bound to the metal surface. It is reasonable to think that the new Cu-AN chemical bonds that are formed prevent AN from translating (diffusion neglected) and rotating on the surface. A consequence of this decrease in the number of degrees of freedom for the [Cu(100)+AN] system is a reduction in entropy upon chemisorption.

When no intermolecular interactions are considered, the thermodynamic properties can be determined from the properties of an isolated molecular system, such as an AN molecule or the [Cu₉-AN] complex. By neglecting the coupling between the electronic, vibrational, translational, and rotational contributions, the entropy modification upon adsorption, ΔS_{ads} , can be written as a sum of three terms:⁵³

$$\Delta S_{\text{ads}} = \Delta S_{\text{vib}} + \Delta S_{\text{trans}} + \Delta S_{\text{rot}} + \Delta S_{\text{elec}}. \quad (3)$$

Note that the electronic contribution is separated from the other ones. For a molecule (AN), this is justified as long as the Born-Oppenheimer approximation is valid. This separation is also applied for the metal cluster. Indeed, although the excited electronic states can probably be reached with thermal energy [$S_{\text{elec}}(\text{Cu}) \neq 0$], the geometry of the metal is probably not affected by this small electronic excitations.

Since it is reasonable to consider that the metal surface does not translate or rotate, and that the chemisorption prevents acrylonitrile from translating and rotating, $\Delta S_{\text{trans}} = S_{\text{trans}}(\text{AN})$ and $\Delta S_{\text{rot}} = S_{\text{rot}}(\text{AN})$. The adsorption should not affect significantly the probability that the metal have to be in some electronic excited states, hence $S_{\text{elec}}(\text{Cu-AN}) = S_{\text{elec}}(\text{Cu})$. Moreover, at room temperature, acrylonitrile is never in an excited state; consequently, the electronic entropy of AN is zero and $\Delta S_{\text{elec}} = 0$. Following this reasonable approximation Eq. (3) becomes

$$\Delta S_{\text{ads}} = [S_{\text{vib}}(\text{Cu-AN}) - S_{\text{vib}}(\text{Cu}) - S_{\text{vib}}(\text{AN})] - S_{\text{trans}}(\text{AN}) - S_{\text{rot}}(\text{AN}). \quad (4)$$

The last two terms are the molar translational entropy and rotational entropy of AN; these contributions to AN total entropy can be evaluated by means of simple models. If AN is considered as a perfect gas of indiscernible particles, the molar translational entropy is expressed as⁵³

$$S_{\text{trans}} = R \ln \left[\left(\frac{2\pi mkT}{h^2} \right)^{3/2} \frac{kT}{P} \right] + \frac{5}{2} R, \quad (5)$$

where m is the molecular mass, P is the pressure of the gas, and T the temperature. For $P=1$ atmosphere and $T=298$ K; the translational entropy of AN is 37.8 cal/mol K.

As far as the rotational contribution is considered, the rigid rotor model can be used to simulate the rotation of AN. If the rotational energy spacings are considered sufficiently small, the molar rotational entropy can be expressed by

$$S_{\text{rot}} = R \ln \left[8 \pi^2 \frac{(2 \pi k T)^{3/2}}{h^3} (I_a I_b I_c)^{1/2} \right] + \frac{3}{2} R, \quad (6)$$

where I_a , I_b , and I_c are the principal moments of inertia of the system. At 298 K, the rotational contribution to entropy is 23.2 cal/mol K for AN. The last contribution is originating from vibrations. In the harmonic oscillator approximation, the molar vibrational entropy is described as

$$S_{\text{vib}} = R \sum_{i=1}^{3n-6} \left[\ln \left(\frac{1}{1 - \exp\left(\frac{-h\nu_i}{kT}\right)} \right) + \frac{h\nu_i}{kT} \frac{\exp\left(\frac{-h\nu_i}{kT}\right)}{1 - \exp\left(\frac{-h\nu_i}{kT}\right)} \right]. \quad (7)$$

A summation must be carried out over all the $3n-6$ modes of vibration, where n is the number of atoms in the molecule. This contribution was evaluated for the AN molecule, the Cu_9 metal cluster modeling the surface, and the $[\text{Cu}_9\text{-AN}]$ complex. Note that for the latter two systems, the negative vibrational frequencies related to imaginary modes were discarded. At 298 K, the vibrational entropy of these systems are $S^{\text{vib}}(\text{AN})=3.8$ cal/mol K; $S^{\text{vib}}(\text{Cu}_9)=64.0$ cal/mol K; and $S^{\text{vib}}(\text{Cu}_9\text{-AN})=65.8$ cal/mol K.

From these results, we see that the major contributions to the entropy decrease come from rotations ($\Delta S_{\text{rot}} = -23.2$ cal/mol K) and translations of AN ($\Delta S_{\text{trans}} = -37.8$ cal/mol K), since these motions are lost upon adsorption. The vibration entropy modification is small: $\Delta S_{\text{vib}} = -2.0$ cal/mol K. As a result, the change in entropy due to chemisorption ΔS_{ads} is equal to -59.0 cal/mol K.

At this point, we can evaluate the free enthalpy modification upon adsorption. The enthalpic contribution can be estimated by the chemisorption energy coming from the DFT calculations (Sec. III D): $\Delta H_{\text{ads}} = -28.0$ kcal/mol. Hence, at 298 K, the free enthalpy of adsorption is calculated to be -10.4 kcal/mol. This result is consistent with the fact that acrylonitrile is chemisorbed on the copper surface under UHV conditions, as shown by the XPS data, and in its liquid phase as observed in the experiments by Loo and Kato.²⁶ The entropic contribution $T\Delta S_{\text{ads}}$ decreases the strength of chemisorption by -17.6 kcal/mol at 298 K; the entropic modification is thus far from being negligible in the chemisorption process (note that the adsorption free enthalpy of acrylonitrile from solution should be smaller than that from gas phase because of the attractive interaction of the surrounding medium composed of solvent and acrylonitrile^{1c}).

IV. CONCLUSION

The chemisorption of the acrylonitrile (AN) monomer is a key step in the electrografting mechanism allowing to form

chemically grafted polyacrylonitrile films onto copper electrodes. In this work, the adsorption of AN on the copper surface has been studied theoretically by means of model copper clusters $\text{Cu}_n(100)$ ranging from 9 to 20 copper atoms interacting with AN, and experimentally with XPS measurements. The theoretical models are studied at the Local Spin Density Approximation of the Density Functional Theory.

The adsorption geometry of AN on Cu(100) is found to be a di- σ chemisorption, where the two terminal atoms of the AN backbone, i.e., a carbon atom and a nitrogen atom, are chemically bound to copper atoms. The fact that the geometry hardly depends on cluster size confirms the local character of the interaction. The correspondence between the calculated vibrational frequencies of AN adsorbed on the model surface and the measured vibrational properties is consistent with the presence of such an adsorbate on the surface of polycrystalline copper electrodes. XPS provides other evidence of acrylonitrile chemisorption on a copper surface and validates our AN/ Cu_n adsorption model, since a qualitative correspondence is found between the changes in XPS binding energies and the calculated atomic charge modifications of AN upon chemisorption.

Since the electronic chemical potential of the copper clusters (which is nearly size independent and close to the Fermi level of copper) is higher than that of AN, chemisorption leads to electron transfer from the clusters or the actual Cu(100) surface toward the AN molecule. This charge transfer is expected to be larger between the actual Cu(100) surface and AN than between small copper clusters and AN, because the hardness of copper clusters significantly decreases with size.

The analysis of the local DOS reveals the molecular orbitals of AN that play an important role in chemisorption. The overlap between $3d$ or $4s$ levels of Cu_{20} and the molecular orbitals of AN can rationalize the chemisorption charge transfer. The local DOS indicate different types of stabilization mechanisms (via the combination of the molecular orbitals of AN and those of the copper cluster), which are favored by the proximity of the electronic levels and thus by a small hardness of the metal cluster.

The chemisorption energy of AN is almost constant with the size of the metal clusters. This allows us to propose an estimate of the enthalpy of chemisorption of AN on Cu(100) on the order of -28 kcal/mol. The weak oscillation of adsorption energy found here differs from that observed in other theoretical studies treating small adsorbate/metal clusters systems; we have pointed out the possible origins of this behavior.

The decrease in the $T\Delta S_{\text{ads}}$ entropy term upon chemisorption of acrylonitrile was evaluated (based on DFT data, using statistical mechanics formulas) to be ≈ -18 kcal/mol at 298 K. The entropic contribution is thus not negligible in the chemisorption process. At 298 K, the free energy of adsorption remains, however, negative (≈ -10 kcal/mol). From the latter result and experimental evidence, we conclude that acrylonitrile chemisorbs on a copper surface. This adsorbate is likely to constitute the actual reactant prior to surface polarization in the electrografting mechanism. We believe that in the electrografting experiment, the adsorbate becomes re-

duced at a given polarization of the metal electrode, reacts with another monomer coming from solution, and propagates the polymerization to lead eventually to a polyacrylonitrile chain grafted to the metal surface.^{1(e)} In a following paper, we will report on a theoretical study of the reduction of chemisorbed acrylonitrile.

ACKNOWLEDGMENTS

The Mons-Saclay collaboration is conducted in the framework of the "TOURNESOL" Belgium—France bilateral project on "Modélisation théorique du greffage de polymères sur des surfaces métalliques." The Mons—Linköping collaboration is supported by the European Commission "Training and Mobility of Researchers (project SELOA)." The work in Mons is partly supported by the Belgian Federal Government "Service des Affaires Scientifiques, Techniques et Culturelles (SSTC)" in the framework of the "Pôle d'Attraction Interuniversitaire en Chimie Supramoléculaire et Catalyse Supramoléculaire (PA1 4/11)" and FNRS-FRFC. XC is a grant holder of "Fonds pour la Formation à la Recherche dans l'Industrie et dans l'Agriculture (FRIA)." RL is Maître de Recherches of the Belgian "Fonds National de la Recherche Scientifique (FNRS)" XC is grateful to the "Ministère de la Communauté Française de Belgique" for a grant that supported his stay in Linköping. WRS thanks the Belgian FNRS for a visiting Professorship at the University of Mons—Hainaut.

- ¹(a) P. Mlynarski and D. R. Salahub, *J. Chem. Phys.* **95**, 6050 (1991); (b) M. A. v. Daelen, Y. S. Li, J. M. Newsam, and R. A. v. Santen, *Chem. Phys. Lett.* **226**, 100 (1994); (c) G. Pacchioni and N. Rösch, *Surf. Sci.* **306**, 169 (1994); (d) M. Weinelt, W. Huber, P. Zebisch, H. P. Steinreck, P. Ulbricht, U. Birkenheuer, J. C. Boettger, and N. Rösch, *J. Chem. Phys.* **102**, 9709 (1995); (e) X. Crispin, R. Lazzaroni, V. Geskin, N. Baute, P. Dubois, R. Jérôme, and J. L. Brédas, *J. Am. Chem. Soc.* **121**, 176 (1999).
²I. Panas, J. Schüle, P. Siegbahn, and U. Wahlgren, *Chem. Phys. Lett.* **149**, 265 (1988).
³V. Russier, D. R. Salahub, and C. Mijoule, *Phys. Rev. B* **42**, 5046 (1990).
⁴X. Crispin, V. Geskin, R. Lazzaroni, C. Bureau, and J. L. Brédas, *Eur. J. Inorg. Chem.* **1999**, 349.
⁵(a) M. D. Morse, M. E. Geusic, J. R. Heath, and R. E. Smalley, *J. Chem. Phys.* **83**, 2293 (1985); (b) M. E. Geusic, M. D. Morse, and R. E. Smalley, *ibid.* **82**, 590 (1985); (c) R. L. Whetten, D. M. Cox, D. J. Trevor, and A. Kaldor, *Phys. Rev. Lett.* **54**, 1494 (1985); (d) J. S. Bradley, J. M. Millar, E. W. Hill, S. Behal, B. Chaudret, and A. Duteil, *Faraday Discuss.* **92**, 255 (1991).
⁶(a) G. Lécayon, Y. Bouizem, C. LeGressus, C. Reynaud, C. Boiziau, and C. Juret, *Chem. Phys. Lett.* **91**, 506 (1982); (b) C. Boiziau and G. Lécayon, *Surf. Interface Anal.* **12**, 475 (1988); (c) G. Tourillon, R. Garrett, N. Lazars, M. Raynaud, C. Reynaud, G. Lécayon, and P. Viel, *J. Electron Spectrosc. Relat. Phenom.* **137**, 2499 (1990); (d) G. Deniau, P. Viel, G. Lécayon, and J. Delhalle, *Surf. Interface Anal.* **18**, 443 (1992); (e) J. Tanguy, P. Viel, G. Deniau, and G. Lécayon, *Electrochim. Acta* **38**, 1501 (1993); (f) J. Tanguy, G. Deniau, C. Augé, G. Zalczer, and G. Lécayon, *J. Electroanal. Chem.* **377**, 115 (1994); (g) R. Jérôme, M. Mertens, and L. Martinot, *Adv. Mater.* **7**, 807 (1995); (h) J. Tanguy, G. Deniau, G. Zalczer, and G. Lécayon, *J. Electroanal. Chem.* **417**, 175 (1996); (i) P. Jonnard, F. Vergand, P. F. Staub, C. Bonnelle, G. Deniau, C. Bureau, and G. Lécayon, *Surf. Interface Anal.* **24**, 339 (1996); (j) M. Mertens, C. Calberg, L. Martinot, and R. Jérôme, *Macromolecules* **29**, 4910 (1996); (k) C. Bureau, G. Deniau, P. Viel, and G. Lécayon, *ibid.* **30**, 333 (1997); (l) M. Mertens, C. Calberg, N. Baute, R. Jérôme, and L. Martinot, *J. Electroanal. Chem.* **441**, 237 (1998).
⁷(a) J. Perreau, C. Reynaud, C. Boiziau, G. Lécayon, C. Makram, and C. L. Gressus, *Surf. Sci.* **162**, 776 (1985); (b) G. Hennico, J. Delhalle, C. Boiziau, and G. Lécayon, *J. Chem. Soc., Faraday Trans.* **86**, 1025 (1990); (c)

- G. Hennico, J. Delhalle, E. Younang, M. Defranceschi, G. Lécayon, and C. Boiziau, *Int. J. Quantum Chem., Quantum Chem. Symp.* **25**, 507 (1991); (d) G. Deniau, G. Lécayon, P. Viel, G. Hennico, and J. Delhalle, *Langmuir* **8**, 267 (1992); (e) C. Bureau, M. Defranceschi, and J. Delhalle, *Int. J. Quantum Chem.* **46**, 87 (1993); (f) C. Bureau and G. Lécayon, *J. Chem. Phys.* **106**, 8821 (1997).
⁸(a) C. Bureau, M. Defranceschi, J. Delhalle, G. Deniau, J. Tanguy, and G. Lécayon, *Surf. Sci.* **311**, 349 (1994); (b) C. Bureau, M. Defranceschi, J. Delhalle, G. Lécayon, and D. R. Salahub, *J. Mol. Struct.* **330**, 279 (1995); (c) C. Bureau, G. Deniau, P. Viel, G. Lécayon, and J. Delhalle, *J. Adhes.* **58**, 101 (1996); (d) C. Fredriksson, R. Lazzaroni, J. L. Brédas, M. Mertens, and R. Jérôme, *Chem. Phys. Lett.* **258**, 356 (1996); (e) V. Geskin, R. Lazzaroni, M. Mertens, R. Jérôme, and J. L. Brédas, *J. Chem. Phys.* **105**, 3278 (1996); (f) X. Crispin, V. Geskin, R. Jérôme, R. Lazzaroni, and J. L. Brédas, in *Proceedings of the 2nd International Conference on Polymer—Solid Interfaces: From Model to Real Systems*, Presses Universitaires de Namur, edited by J. J. Pireaux, J. Delhalle, and P. Rudolf (Namur, Belgique, 1996), pp. 53–64.
⁹R. A. Bradley, R. Georgiadis, S. D. Kevan, and G. L. Richmond, *J. Chem. Phys.* **99**, 5535 (1993).
¹⁰R. G. Parr and W. Yang, *Density-Functional Theory of Atoms and Molecules* (Oxford University Press, New York, 1989), p. 225.
¹¹D. P. Chong, *Recent Advances in Density Functional Methods* (World Scientific, Singapore, 1995), Vol. 1.
¹²B. Delley, *J. Chem. Phys.* **92**, 508 (1990).
¹³B. Delley, *New J. Chem.* **16**, 1103 (1992).
¹⁴MSI. DMol 96.0/4.0.0, *Quantum Chemistry User Guide*, San Diego, 1996.
¹⁵D. Ellis and G. Painter, *Phys. Rev. B* **2**, 2887 (1968).
¹⁶H. Vosko, L. Wilk, and M. Nusair, *Can. J. Phys.* **58**, 1200 (1980).
¹⁷(a) J. Baker, *J. Comput. Chem.* **7**, 385 (1986); (b) J. Baker and W. J. Hehre, *ibid.* **12**, 606 (1991); (c) J. Baker, *ibid.* **13**, 240 (1992); (d) J. Baker, *ibid.* **14**, 1085 (1993).
¹⁸B. Delley, M. Wrinn, and H. P. Lüthi, *J. Chem. Phys.* **100**, 5785 (1994).
¹⁹T. Ziegler, *Chem. Rev.* **91**, 651 (1991).
²⁰F. L. Hirshfeld, *Theor. Chim. Acta* **44**, 129 (1977).
²¹B. Delley, *Chem. Phys.* **110**, 329 (1986).
²²E. B. J. Wilson, J. C. Decius, and P. C. Cross, *Molecular Vibrations* (Dover, New York, 1980).
²³I. Papai, A. St-Amant, and D. Salahub, *Surf. Sci.* **240**, L604 (1990).
²⁴M. A. v. Daelen, Y. S. Li, J. M. Newsam, and R. A. v. Santen, *Chem. Phys. Lett.* **226**, 100 (1994).
²⁵R. Fournier and I. Papai, in *Recent Advances in DFT Methods. Part 1*, edited by D. Chong, Singapore, 1995, pp. 219–285.
²⁶B. H. Loo and T. Kato, *Surf. Sci.* **284**, 167 (1993).
²⁷F. Halverson, R. F. Stamm, and J. J. Whalen, *J. Chem. Phys.* **16**, 808 (1948).
²⁸D. Becke, *Phys. Rev. A* **38**, 3098 (1988).
²⁹J. P. Perdew and Y. Wang, *Phys. Rev. B* **45**, 13 244 (1992).
³⁰M. D. Morse, J. B. Hopkins, P. R. R. Langridge-Smith, and R. E. Smalley, *J. Chem. Phys.* **79**, 5316 (1983).
³¹R. Fournier, *J. Chem. Phys.* **98**, 8041 (1993).
³²S. K. So, R. Franchy, and W. Ho, *J. Chem. Phys.* **95**, 1385 (1991).
³³M. H. Mohamed and L. L. Kesmodel, *Surf. Sci.* **185**, L467 (1987).
³⁴(a) A. Naves de Brito, S. Svensson, H. Ågren, and J. Delhalle, *J. Electron Spectrosc. Relat. Phenom.* **63**, 239 (1993); (b) Bureau, D. P. Chong, G. Lécayon, and J. Delhalle, *ibid.* **83**, 227 (1997).
³⁵(a) R. F. Nalewajski, *J. Am. Chem. Soc.* **106**, 944 (1984); (b) W. J. Mortier, S. K. Ghosh, and S. Shankar, *ibid.* **108**, 4315 (1986); (c) R. G. Parr and R. G. Pearson, *ibid.* **105**, 7512 (1983); (d) R. G. Parr and W. Yang, *ibid.* **106**, 4049 (1984); (e) W. Yang, R. G. Parr, and R. Pucci, *J. Chem. Phys.* **81**, 2862 (1984).
³⁶The term containing the variation of the external potential Δv_{AN} is expected to have the same order of magnitude whatever the size of the clusters (provided it is reasonably large) since only part of the cluster surface localized around the adsorbate is involved in the chemisorption. The product $[f_{Cu_i}(r)\Delta v_{Cu_i}(r)]$ has a significant value only in the region of chemisorption and the Fukui function of a cluster is already a good estimate of that of the metal for the region in interaction with AN; hence, this term should be of the same order of magnitude whatever the size of the cluster.
³⁷J. Cioslowski and B. B. Stefanov, *J. Chem. Phys.* **99**, 5151 (1993).
³⁸A. B. Anderson, *J. Chem. Phys.* **68**, 1744 (1978).
³⁹J. M. Burkstrand, G. G. Kleiman, G. G. Tibbets, and J. C. Tracy, *J. Vac. Sci. Technol.* **13**, 291 (1976).

- ⁴⁰P. O. Löwdin, *J. Chem. Phys.* **18**, 365 (1950).
- ⁴¹R. Hoffmann, *Solids and Surfaces: A Chemist's View of Bonding in Extended Structures* (VCH, New York, 1988).
- ⁴²G. te Velde and E. J. Baerends, *Chem. Phys.* **177**, 399 (1993).
- ⁴³K. Hermann, P. S. Bagus, and C. J. Nelin, *Phys. Rev. B* **35**, 9467 (1987).
- ⁴⁴M. Matos and B. Kirtman, *Surf. Sci.* **341**, 162 (1995).
- ⁴⁵C. Mijoule, M. F. Baba, and V. Russier, *J. Mol. Catal.* **83**, 367 (1993).
- ⁴⁶G. Klopman and R. F. Hudson, *Theor. Chim. Acta* **8**, 165 (1967).
- ⁴⁷I. Panas and P. E. M. Siegbahn, *J. Chem. Phys.* **92**, 4625 (1990).
- ⁴⁸A. Vela and J. L. Gazquez, *J. Am. Chem. Soc.* **112**, 1490–1492 (1990).
- ⁴⁹P. E. M. Siegbahn, L. G. M. Pettersson, and U. Wahlgren, *J. Chem. Phys.* **94**, 4024 (1991).
- ⁵⁰L. M. Falicov and G. A. Somorjai, *Proc. Natl. Acad. Sci. USA* **82**, 2207 (1985).
- ⁵¹W. Yang and R. G. Parr, *Proc. Natl. Acad. Sci. USA* **82**, 6723 (1985).
- ⁵²Note that for finite metal clusters taken as surface models, the Fukui function is located on the edge of the cluster.^{8(c)} As a consequence, the edge atoms would be the preferential sites for chemisorption; however, since these edge atoms are not representative of metal surface atoms, we have not brought AN into an interaction with the edge atoms but rather with the central atoms, that have the same saturation as the actual metal surface atoms. The Fukui function of the cluster near these central atoms is expected to be closer to that of the actual Cu(100) surface.
- ⁵³R. S. Berry, S. A. Rice, and J. Ross, *Physical Chemistry* (Wiley, New York, 1980).